Multiple Sulfidation/Regeneration Cycle Tests for Advanced Fuel Conversion Process by 20 wt%Fe2O3/Al2O3 Sorbent

Huang, C.Y.
2014

Multiple Sulfidation/Regeneration Cycle Tests for Advanced Fuel Conversion Process by 20 wt%Fe_2O_3/Al_2O_3 Sorbent

C.Y. Huang, Y. P. Chyou, [1] K. Svoboda
Institute of Nuclear Energy Research, Chemistry Division, No. 1000, Wenhua Rd., Jiaan Village, Longtan Township, Taoyuan County 32546, Taiwan (R.O.C.) ;
Tel.: +886 3 4711400 x. 5058, E-mail: huangjy7215@gmail.com; Tel.: +886 34711400 x. 5050, E-mail: ypchyou@iner.gov.tw, fax: +886 34711412.
[1]Institute of Chemical Process Fundamentals of the ASCR, v.v.i., Rozvojová 135, 165 02 Prague 6, Czech Republic;
Tel.: +420 220 390 160; E-mail: svoboda@icpf.cas.cz; Fax: +420 220 920 661

O

ver the past decade, coal remained the largest energy source for global power generation and supplied the largest share of additional electricity generated to meet demand worldwide, which inevitably led to larger amounts of CO_2 released into the atmosphere. This trend must be subdued or even reversed by reducing CO_2 emissions in the power sector. An enhanced power generation efficiency, a switch to lower-carbon fossil fuels, an increased utilization of renewables and nuclear power, and the introduction of CCS (carbon capture and storage) are possible options to achieve this objective. At present, many countries concentrate their attention to the development of clean coal technologies to enhance the efficiency and the environmental benignity of coal extraction, preparation, and utilisation, among which gasification illustrates a paradigm of BACT (best achievable control technology) concept. Dry sulfidation technology in coal gasification plants can be implemented to prevent the sulfur corrosion of equipment and reduce pollutant emissions to meet environmental regulations and improve energy efficiency.

I

n this study, 20 wt%Fe_2O_3/Al_2O_3 was used as a sorbent to perform multiple sulfidation/regeneration cycle tests in a fixed-bed reactor under simulated hot syngas conditions (For the sulfidation step: 973K, inlet gases:CO:30%, H_2S:1%, CO_2:5%, H_2:10%, N_2 balance; For the regeneration step: Air, 973K). The physical properties of sorbents were analyzed by X-ray diffraction (XRD), inductively coupled plasma atomic emission spectrometry (ICP-AES), BET, and SEM/EDS. ICP-AES results indicated that the composition of metal oxide was close to the theoretical value. Multiple sulfidation/regeneration cycle tests showed that the 20wt%Fe_2O_3/Al_2O_3 can be regenerated and thus reused after the oxidation process. Due to the sulfidation reaction, colour change of the 20 wt%Fe_2O_3/Al_2O_3 sorbent was observed, from the original red to black. After six sulfidation-regeneration cycles, the sulfur capacity of the sixth cycle remained approximately on a level of 68% of the sulfur capacity in the first cycle. The BET analysis showed that the surface area decreased as the cycle number increased. The sulfidation-regeneration cycles were coupled with endothermic-exothermic reactions, which probably caused sintering of the sorbent, decreasing its surface area and sulfur capacity.

a high-temperature, high-pressure reactor to run multiple cycle tests will be established.

Introduction

In recent years, the integrated gasification combined cycle (IGCC) is one of the most promising clean coal technologies that not only improve the thermal efficiency but also eliminate or reduce environmentally harmful pollutants. In an IGCC system, coal-derived syngas contains several low concentrations of impurities, such as H_2S, dust, HCl, and NH_3. The concentration of hydrogen sulfide (H_2S) varies with feedstock and gasifier type, ranging from 0.2~1.4% [1-3]. The sulfur compounds (H_2S & COS) in coal-derived syngas not only contribute to environmental pollution but also induce corrosion. Therefore, the development of high-temperature desulfurization technology is very important for IGCC power generation systems.

In the last few decades, many researchers have devoted attention to the research and development of regenerable sorbents for high-temperature processes. Candidate sorbents for hot-gas desulfurization should meet several requirements, which include higher sulfur capacity, regeneration efficiency, mechanical stability, chemical stability, etc., through multiple sulfidation/regeneration cycle tests, as mentioned in the literature [4]. There are many kinds of metal-oxides that have been studied to remove H_2S, such as zinc oxide, copper oxide, manganese oxide, iron oxides [5-8], zinc ferrite, zinc titanate, etc. In addition, in order to resolve problems about sintering, low utilization of active compound, and attrition of sorbents, the metal oxide is usually supported on TiO_2, Al_2O_3, ZrO_2 and zeolite to increase the stability of the sorbent, but with decreased sulfur capacity.Selecting a sorbent candidate depends on the material's chemical and physical properties. Zinc oxide owns superior thermodynamic properties to reach lower outlet H_2S concentration and has been developed in a variety of commercial sorbents [9-12], such as Z-Sorb III, RVS-1, RTI-3, etc. However, Zinc-oxide sorbent is easily evaporated at high temperatures in reductive atmospheres, so the operating temperature needs to be below 600°C. Copper oxide has good thermodynamic properties that could reduce sulfide concentration emission [13], but it cannot endure reducing atmospheres at high temperature, usually above 800°C, without being reduced to a low oxidation number state [14], Cu_2O or Cu, that could result in a loss of reactivity. In order to improve the stability of copper oxide, it is suggested to add Cesium or Cerium element [15]. The manganese-based sorbent has high sulfur capacity and good regenerative ability during hot gas desulfurization at 700-1000°C. It is usual to add iron oxide [16], zinc oxide [17], and copper oxide [18] to increase the H_2S removal efficiency. Iron oxide sorbent has been used favorably because of its high sulfur capacity and reactivity as well as its ease of regeneration [19]. Besides, iron oxides come from cheap and abundant precursor materials such as iron ore and red mud in comparison with others.

Experimental

Sorbent preparation and characterization

The Iron(III)-nitrate (Alfa-Aesar, $Fe(NO_3)_3 \cdot 9H_2O$, 99.5%) was used to prepare the sorbent. Alumina (Alfa-Aesar) was used as a support in this study. Sulfidation sorbent was prepared by the impregnation method. Ten grams of alumina were ground up and sieved through 300 and 600 μm (30~50 meshes). Then, it was dried at 373K to deplete moisture before synthesis. The sorbent of 20wt%Fe_2O_3/Al_2O_3 was synthesized by mixing 12.86 g $Fe(NO_3)_3 \cdot 9H_2O$ with suitable amounts of DI-Water, and then the solution was poured onto the alumina support. The impregnated alumina support was left to stand overnight at room temperature and dried in an oven for 24 hours to remove additional moisture. The precursor was calcinated at 973K for 6 hours to synthesize the required sorbent.

Characterization of the 20 wt%Fe_2O_3/Al_2O_3 sorbent

-ray diffraction was conducted to obtain structural information about freshly synthesized and post-reaction sorbent samples by a XRD analyzer (Bruker-D8-ADVANCE X-ray diffraction with CuKα radiation). The scanning rate 2°/min with a scanning range from 20° to 80° were used, and the crystalline phases were identified using JCPDS files. The surface area of the sorbent was measured with a Micromeritics ASAP 2020 instrument using adsorption of nitrogen at 77K. Prior to adsorption measurements, the samples were degassed under a vacuum of 5 μmHg at 383K for 3 hrs. The surface area was calculated by the BET equation. The practical metal loading of high temperature calcined sulfidation sorbent was analyzed by an ICP (Inductively coupled plasma; JOBIN YVON JY38S) analyzer.

The chemical performance evaluation of the sulfidation sorbent was performed by a fixed-bed reactor and a gas chromatograph (Varian 450 GC) equipped with a pulse flame photometric detector (PFPD) and fitted with a GS-Q capillary column. The fixed-bed reactor system was shown in Figure 1. The operating parameters of the desulfurization reaction were chosen according to the previous experimental results, which discussed the impact of different compositions of syngas on the sulfur capacity of the 20 wt%Fe_2O_3/ Al_2O_3 sorbent [20]. The operation parameters used for the evaluation tests are shown in the Table 1.

Table 1 Target test conditions during sulfidation and regeneration experiment

Parameter	Operation condition
Sulfidation temperature	973K
Regeneration temperature	973K
Inlet sulfidation composition	10%H_2; 30%CO; 1%H_2S; 5%CO_2; N_2 balance
Inlet regeneration composition	Air
Weight hourly space velocity	8,000 mL/hr-g
Load weight of sorbent	1.5 g
Sorbent size	300-600 μm (30~50 meshes)

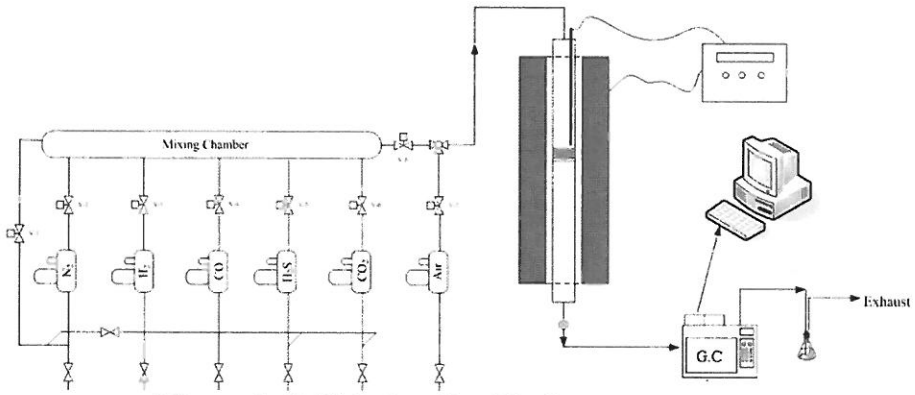

Figure 1. Sulfidation fixed-bed reactor system

Results and Discussion

The physical properties of 20 wt%Fe_2O_3/Al_2O_3 sorbent

Table 2 shows the basic physical properties of the 20 wt%Fe_2O_3/Al_2O_3 sorbent. Inductively coupled plasma (ICP) spectroscopy is adopted to analyze metal contents, which determined the metal-oxide loading of the 20 wt%Fe_2O_3/Al_2O_3 sorbent. It revealed that metal oxide recovery of the sulfidation sorbent was close to the nominal value. The results of the BET analysis showed that the 20 wt%Fe_2O_3/Al_2O_3 sorbent calcinated over 973K for 6 hours still had high surface area. The BET surface area of the sorbent was 119.04 m^2/g. This characteristic could be beneficial to increased gas-solid contacting opportunity.

In order to understand the crystalline phase of the sorbent, a sample was grounded and analyzed by XRD. The XRD result was compared with the standard patterns from JCPDS files. The sample of 20 wt%Fe_2O_3/Al_2O_3 was inspected to have Fe_2O_3 and Al_2O_3 phases, as shown in Figure 2. The result also showed that the objective crystalline phase could be achieved at this synthesizing condition.

Table 2. The basic properties of the 20 wt%Fe_2O_3/Al_2O_3 sorbent

Sorbent	Fe_2O_3 loading (%)	BET surface area (m^2/g)
20 wt%Fe_2O_3/Al_2O_3	19.34	119.04

EMBED SigmaPlotGraphicObject.9

Figure 2. XRD pattern of 20 wt%Fe_2O_3/Al_2O_3 sorbent

Multiple sulfidation/regeneration cycle tests

The homemade 20wt%Fe_2O_3/Al_2O_3 sorbent could be repeatedly re-used after regenerah curves of the six sulfidation-regeneration cycles with the 20wt%Fe_2O_3/Al_2O_3 sorbent at 700°C are presented in Figure 3. Figure 3 shows that before breakthrough, the sorbent reduced the H_2S to low concentrations in every sulfidation reaction. The slope of each breakthrough curve was very steep, which meant that the gas-solid reaction occured quickly. Referring to COP Z-SorbIII application, 500 ppmv was defined as the breakthrough point. The actual sulfur capacity (M_{H2S}) is expressed in the formula (1) as below [21],

$$M_{H2S} = \left(MW_{H2S} \times \frac{PF_{gas} y_{H2S}}{R_g T} \right) \times t_s \quad (1)$$

where M_{H2S} is the mass of the actual sulfur captured by the sorbent, MW_{H2S} is the molecular weight of H_2S, P is the absolute pressure, F_{gas} is the volumetric gas flow rate under the process condition, y_{gas} is the inlet H_2S mole fraction, R_g is the universal gas constant, T is the absolute temperature, and t_s is the actual sulfidation time until breakthrough (typically 500 ppm).

The breakthrough time (In this study, defined as the amount of time it takes for the H_2S concentration to reach 500ppm) is also used to evaluate the sulfur capacity of the 20wt %Fe_2O_3/Al_2O_3 sorbent before H_2S breakthrough. The breakthrough times and sulfur capacities of the six sulfidation-regeneration cycles are shown in Figure 4. It is indicated that sulfur capacity and breakthrough time dropped sensibly from the first to the fourth cycle and then kept at a constant value. The initial sulfur capacity was 4.47 g-S/100g sorbent; then it

decreased to 3.6 g-S/100g sorbent between the second and the fourth cycle; it finally maintained a constant level at 3.08 g-S/100g sorbent after the fifth cycle. The sulfur capacity of the sixth cycle dropped to 68% of the initial performance. The reasons for the activity decay will be discussed in later physical property studies.

EMBED SigmaPlotGraphicObject.9

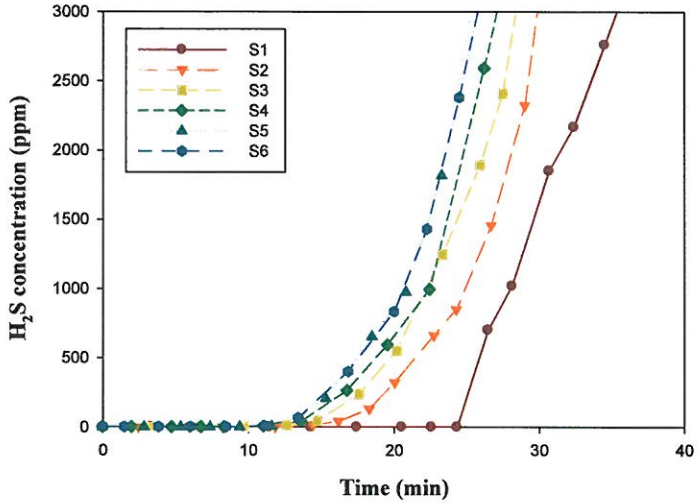

Figure 3. The breakthrough curves of the six sulfidation-regeneration cycles

EMBED SigmaPlotGraphicObject.9

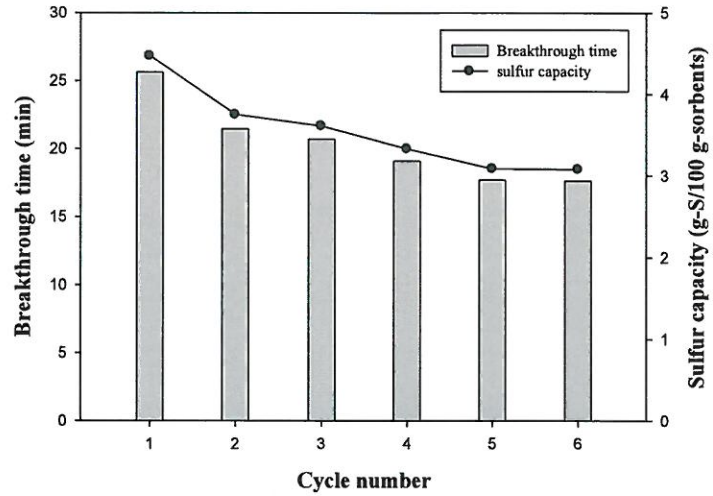

Figure 4. The breakthrough times and sulfur capacities of the sixs

Figure 5(a) shows the XRD pattern of the sulfided 20wt%Fe_2O_3/Al_2O_3 sorbent; whatlline phase of the sulfided sorbent was mainly composed of FeS and γ-Al_2O_3. It represents that while the iron-oxide sorbent was transformed into FeS after the sulfidation reaction, the Al_2O_3 support did not join the reaction as well. The XRD patterns of the fresh and regenerated 20wt %Fe_2O_3/Al_2O_3 sorbent were shown in Figure 5(b). It could be clearly shown that during regeneration, the sorbent reacts with air and returns to the original crystalline phase to achieve a successful multiple sulfidation-regeneration cycle test. In addition, the $FeSO_4$ phase didn't exist in the regenerated sorbent.

EMBED SigmaPlotGraphicObject.9

EMBED SigmaPlotGraphicObject.9

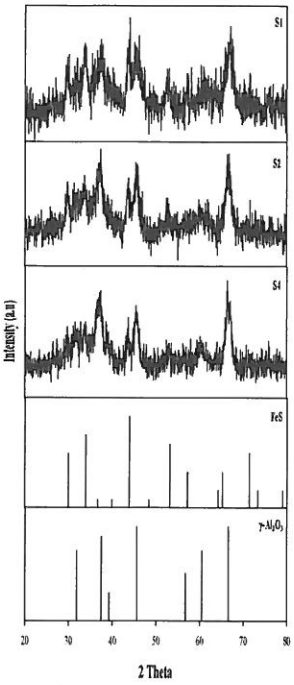

(a) Sulfided sorbent **(b) Fresh & regenerated sorbent**

Figure 5. XRD patterns of different statuses of 20 wt%Fe_2O_3/Al_2O_3 sorbent

The surfacewerebased on the BET equation and summarized in Table 3. After comparing fresh and after-1st-sulfurization-reaction sorbents, it was found that the BET surface area of the sulfided sorbent decreased. The reason was that during the sulfidation reaction, where the Fe_2O_3 reacted with H_2S, the S ions substituted for the O atoms in the lattice of the Fe_2O_3 crystal structure. This caused the expansion of the unit cell, because the ionic radii of the O^{2-} and S^{2-} anions are 1.4 and 1.84Å, respectively. The grains of Fe_2O_3 in the sorbent became bigger after reaction with H_2S, which may have caused pore volume to decrease and pore size to increase [22]. The multiple-cycle reactions are endothermic-exothermic reactions at high temperature, which may have caused 20wt%Fe_2O_3/Al_2O_3 sorbent sintering. From Table 3, it was found that a substantial loss of the BET surface area and pore volume was observed after six sulfuration-regeneration cycle test.

From Figure 6, the 20wt%Fe_2O_3/ Al_2O_3 sorbent and after-sulfidation–reaction sorbent exhibited a Type IV adsorption isotherm. This adsorption characteristic was usually attributed to adsorption in mesopores, which were classified by IUPAC as pores of diameter 2~50 nm [23]. The gas was adsorbed inside the pores of the material forming first a monolayer and then a multilayer, with capillary condensation finally taking place. The Type IV isotherm includes the following features: at low pressure, the isotherm follows the same path as a Type II isotherm, but at a certain point it begins to deviate upwards, until, at high pressures, its slope decreases [24].

SEM morphologies of fresh, sulfided, and regenerated sorbents are shown in Figure 7. From Figure 7(a) and (b), it is clear that the surface of the sorbent has drastically changed after high-temperature sulfidation. This could be attributed to iron-oxide reaction with hydrogen sulfide to produce iron sulfide. There were many dense particles distributed on the surface of the sulfided sorbent. As the sulfidation-regeneration cycle number increased, the particles agglomerated on the surface, which became noticeably different from the fresh sorbent. This might be due to a high-temperature sintering effect, which may be observed clearly from the BET analysis results above.

In order to identify the elements that existed in fresh, sulfided, and regenerated sorbents, energy dispersion spectrum (EDS) analysis was utilized to perform semi-quantitative element analysis. The results are shown in Table 4. Theresult shows that the sulfur capacities of the sulfided sorbent are consistent with the breakthrough time calculated. The results demonstrate that the 20wt%Fe_2O_3/Al_2O_3 sorbent can sucessfully adsorb hydrogen sulfide and regenerate with air to return to a relatively fresh status. After the 6th regeneration reaction, trace amounts of sulfur were present in the regenerated sorbent, which might be a reason for activity decay.

Table 3. BET surface area of different-status 20 wt%Fe_2O_3/Al_2O_3 sorbents LINK Excel.Sheet.12 L:\\103 實驗數據\\BET\\BET 統整表.xlsx BET 總表!R5C4:R12C7 \a \f 4 \h * MERGEFORMAT

	Surface area (m^2/g)	Pore volume (cm^3/g)	Pore size (Å)
20FA-Fresh	137.89	0.56	63.02
20FA-S1	122.38	0.53	68.05
2t			

Table 4. The semi-quantitative element analysis of fresh, sulfided, and regenerated 20wt %Fe_2O_3/Al_2O_3 sorbents by EDS analyzer

Element	Weight (%)			
	Fresh	S1	S4	R6
C	2.34	-	-	-
O	52.46	40.01	50.39	46.75
Al	35.86	41.69	35.66	39.44
Fe	9.33	13.94	10.07	13.37
S	-	4.35	3.88	0.44

Conclusions

A high surface area for 20wt%Fe_2O_3/Al_2O_3 sorbent was successfully prepared by wet incipient method. The sorbent was capable of removing H_2S to below 500 ppm before the breakthrough point at 700°C in simulated syngas and could be regenerated with air to achieve multiple desulfurization-regeneration cycles. From six desulfurization-regeneration cycle tests, it was found that the sulfur capacity decreased as the cycle test number increased. The initial sulfur capacity of the 20wt% Fe_2O_3/Al_2O_3 sorbent was 4.47 g-S/100g sorbent, which decreased to 3.08 g-S/100g-sorbent after several sulfidation and regeneration cycles. From the analysis of BET and SEM, a sintering effect was suggested as the cause of particle

agglomeration that decreased pore area and pore volume of the sorbent. After the 6th regeneration reaction, there was 0.44% sulfur present in the regenerated sorbent. This study found that high-temperature sintering and full or partial regeneration were the most important and likely factors that affected activity decay.

Acknowledgements
The authors appreciate financial support from the Grant Agency of Czech Republic (GAČR), bilateral grant project of GAČR and National Science Council (NSC) Taiwan, Registr. No. in CR: 14-09692J (Registr. No of foreign project 102WBS0300011) and Grant No. in Taiwan: NSC 103-2923-E-042A-001 -MY3.

Reference

1] Cayan F., Zl

2] EG&G Tech

3] Gupta R., O

4] Williams B.

5] Westmorela

6] Ben-Sliman

7] Pineda M., I

8] Karvan O., S

9] Flytzani-Ste

10] Sánchez-H

11] Siriwardan
(US), 2001.

12] RTI Interna

13] Flytzani-St

14] Case G. D.

15] Li Z., Flytz

16] Zhang J., V

17] Alonso L.,

18] Alonso L.,

19] Zhang J., V

20] Huang C. Y

21] Sánchez J.

22] Novochins
Fuel, 2004; 18,

23] Rouquerol
1758.

24] Aligizaki K

HYPERLINK "http://books.google.com.tw/books?id=P-DGDRfAk8MC&pg=PA114&lpg=PA114&dq=Type+IV+Isotherm&source=bl&ots=79GBm6DGNG&sig=_sDdoB4eWe4AOs7LAmqEiPKGZTw&hl=zh-TW&sa=X&ei=dFUmU5v4KIL2lAWetYBI&ved=0CHcQ6AEwCg" \l "v=onepage&q=Type%20IV%20Isotherm&f=false [accessed"http://books.google.com.tw/books?id=P-DGDRfAk8MC&pg=PA114&lpg=PA114&dq=Type+IV+Isotherm&source=bl&ots=79GBm6DGNG&sig=_sDdoB4eWe4AOs7LAmqEiPKGZTw&hl=zh-TW&sa=X&ei=dFUmU5v4KIL2lAWetYBI&ved=0CHcQ6AEwCg#v=onepage&q=Type%20IV%20Isotherm&f=false [accessed in Apri. 9, 2014]

EMBED Equation.3 $M_{N2} = \left(MW_{\text{[illegible]}} \times \frac{PF_{ad,N2} V_{N2}}{R_t T} \right) \times t_s$